PCP
PLANT & CELL PHYSIOLOGY

Special Focus Issue – Regular Paper

# Using GCaMP3 to Study $Ca^{2+}$ Signaling in *Nicotiana* Species

Thomas A. DeFalco[1,6], Masatsugu Toyota[2,3,4], Van Phan[1], Purva Karia[1], Wolfgang Moeder[1], Simon Gilroy[2] and Keiko Yoshioka[1,5,*]

[1]Department of Cell & Systems Biology, University of Toronto, Toronto, M5S 3B2, Canada
[2]Department of Botany, University of Wisconsin, Madison, WI 53706, USA
[3]Department of Biochemistry and Molecular Biology, Saitama University, 255 Shimo-Okubo, Sakura-ku, Saitama, 338-8570, Japan
[4]Japan Science and Technology Agency (JST), Precursory Research for Embryonic Science and Technology (PRESTO), 4-1-8 Honcho, Kawaguchi, Saitama, 332-0012 Japan
[5]Center for the Analysis of Genome Evolution and Function (CAGEF), University of Toronto, Toronto, M5S 3B2, Canada
[6]Present address: The Sainsbury Laboratory, Norwich NR4 7UH, UK.
*Corresponding author: Email; keiko.yoshioka@utoronto.ca; Fax, +1 416-978-5878.
(Received November 14, 2016; Accepted April 6, 2017)

**$Ca^{2+}$ signaling is a central component of plant biology; however, direct analysis of *in vivo* $Ca^{2+}$ levels is experimentally challenging. In recent years, the use of genetically encoded $Ca^{2+}$ indicators has revolutionized the study of plant $Ca^{2+}$ signaling, although such studies have been largely restricted to the model plant Arabidopsis. We have developed stable transgenic *Nicotiana benthamiana* and *Nicotiana tabacum* lines expressing the single-wavelength fluorescent $Ca^{2+}$ indicator, GCaMP3. $Ca^{2+}$ levels in these plants can be imaged *in situ* using fluorescence microscopy, and these plants can be used qualitatively and semi-quantitatively to evaluate $Ca^{2+}$ signals in response to a broad array of abiotic or biotic stimuli, such as cold shock or pathogen-associated molecular patterns (PAMPs). Furthermore, these tools can be used in conjunction with well-established *N. benthamiana* techniques such as virus-induced gene silencing (VIGS) or transient heterologous expression to assay the effects of loss or gain of function on $Ca^{2+}$ signaling, an approach which we validated via silencing or transient expression of the PAMP receptors FLS2 (Flagellin Sensing 2) or EFR (EF-Tu receptor), respectively. Using these techniques, along with chemical inhibitor treatments, we demonstrate how these plants can be used to elucidate the molecular components governing $Ca^{2+}$ signaling in response to specific stimuli.**

**Keywords:** GCamP3 • CNGC • Calcium • Nicotiana • VIGS • PAMP.

**Abbreviations:** CaM, calmodulin; CNGC, cyclic nucleotide-gated channel; DAMP, damage-associated molecular pattern; DPI, diphenyleneiodonium; EFR, EF-Tu receptor; EF-Tu, elongation factor-Tu; FLS2, Flagellin Sensing 2; GECI, genetically encoded calcium indicator; GFP, green fluorescent protein; PAMP, pathogen-associated molecular pattern; PCD, programmed cell death; PDS, phytoene desaturase; PLC, phospholipase C; PTI, pattern-triggered immunity; ROS, reactive oxygen species; TEV, *Tobacco etch virus*; TMV, *Tobacco mosaic virus*; TRV, *Tobacco rattle virus*; VGCC, voltage-gated calcium channel; VIGS, virus-induced gene silencing.

## Introduction

$Ca^{2+}$ functions as a near-universal second messenger in eukaryotes (Clapham 2007). In particular, $Ca^{2+}$ signaling has taken on astounding complexity in multicellular organisms such as plants, where it mediates responses to diverse stimuli (Sanders et al. 2002, Kudla et al. 2010). Rapid and transient changes in $Ca^{2+}$ concentration within the cell are thought to be sensed by a large suite of $Ca^{2+}$-binding sensor proteins (DeFalco et al. 2010, Batistič and Kudla 2012), and as such there has long been an interest in methods to monitor $Ca^{2+}$ levels within the cell over time at high temporal resolution. $Ca^{2+}$-sensitive fluorescent dyes such as fura-2 or indo-1 were utilized for this purpose for many years (Grynkiewicz et al. 1985, Steinhorst and Kudla 2013), though their use is ultimately limited by the need to deliver the dye into the cytosol (Tian et al. 2012, Rose et al. 2014). This difficulty was partially resolved with the use of aequorin-expressing transgenic organisms (Gilroy et al. 1989, Knight et al. 1993, Whitaker 2012), though $Ca^{2+}$-dependent aequorin luminescence requires the presence of its cofactor coelenterazine, which must be supplied exogenously (Knight and Knight 1995, Toyota et al. 2013).

The development of fluorescence-based genetically encoded $Ca^{2+}$ indicators (GECIs) has since revolutionized the study of $Ca^{2+}$ signaling in eukaryotes by allowing for the observation of dynamic *in vivo* $Ca^{2+}$ flux *in situ* without the need to apply substrates and at high resolution at the cellular level (Miyawaki et al. 1997, Tian et al. 2012, Whitaker 2012, Rose et al. 2014). Generally, these sensors rely on chimeric fusions of one or more fluorescent proteins to the $Ca^{2+}$-binding protein calmodulin (CaM) and a $Ca^{2+}$-dependent CaM-binding M13 peptide. In the case of ratiometric sensors such as cameleons, a $Ca^{2+}$-dependent Förster resonance energy transfer (FRET) effect allows for the *in vivo* $Ca^{2+}$ concentration to be calculated from the ratio between two emission wavelengths (Nagai et al. 2004, Monshausen 2012, Whitaker 2012). Alternatively, other sensors such as the GCaMPs are intensity based, and show increased fluorescence upon $Ca^{2+}$ binding at physiological concentrations (Nakai et al. 2001). With respect to plant biology, studies utilizing GECIs have been largely restricted to the model plant

*Plant Cell Physiol.* 58(7): 1173–1184 (2017) doi:10.1093/pcp/pcx053, Advance Access publication on 8 May 2017, available online at www.pcp.oxfordjournals.org

Arabidopsis (Monshausen 2012), where both cameleons (Choi et al. 2014) and single-wavelength reporters (*i.e.* single-FP GECIs) such as R-GECOs (Zhu et al. 2014, Keinath et al. 2015) or Cases (Souslova et al. 2007) have been used to study $Ca^{2+}$ signals in response to specific stimuli.

Both tobacco (*Nicotiana tabacum*) and its relative *Nicotiana benthamiana* are well established as tools for research use for a variety of reasons, such as their susceptibility to many viruses and their amenability to *Agrobacterium*-mediated transient expression of heterologous genes. For this reason, *N. benthamiana* in particular has become a workhorse of plant research (Goodin et al. 2008) and, as such, we set out to develop methods to analyze $Ca^{2+}$ signals in this plant. While most measurements of $Ca^{2+}$ signals in plants have been restricted to Arabidopsis, recent work has also been performed in other species including rice, *Lotus* and *Medicago* (Sieberer et al. 2009, Krebs et al. 2012, Behera et al. 2015). Additionally, some work has been performed with *N. benthamiana* (Zhu et al. 2010, Segonzac et al. 2011), including experiments utilizing transgenic *N. benthamiana* expressing aequorin to quantify $Ca^{2+}$ responses during pattern-triggered immunity (PTI) and evaluate the roles of various signaling components (Segonzac et al. 2011). However, visualization by aequorin relies on the presence of coelenterazine, making *in situ* measurements difficult, and requires a highly sensitive luminescence detection system such as an image-intensified photon-counting camera (Toyota et al. 2007). Thus, we have endeavored to develop a versatile system that allows for fluorescence-based visualization and measurement of $Ca^{2+}$ signals in response to diverse stimuli in *Nicotiana* species. Here we describe the development of such a system, using transgenic *N. tabacum* and *N. benthamiana* plants stably overexpressing the single-wavelength, fluorescence intensity GECI, GCaMP3 (Tian et al. 2009), a sensor featuring circularly permutated green fluorescent protein (GFP) flanked by CaM and the $Ca^{2+}$-dependent CaM-binding peptide M13. In the absence of $Ca^{2+}$, GCaMP3 has low fluorescence, which increases upon reversible $Ca^{2+}$ loading of the CaM domain as $Ca^{2+}$ levels rise. GCaMP3 functions at physiologically relevant pH and $Ca^{2+}$ levels ($K_d$ approximately 330 nM) (Helassa et al. 2015), making it an excellent tool for the analysis of *in planta* signals. In the case of *N. tabacum*, we have generated transgenics in both the *Tobacco mosaic virus* (TMV)-susceptible [*N. tabacum* cv. Xanthi (nn) (hereafter referred to as nn)] and TMV-resistant [*N. tabacum* cv. Xanthi-nc (NN) (hereafter referred to as NN)] cultivars (Holmes 1954, Erickson et al. 1999).

Our GCaMP3 *Nicotiana* plants can be analyzed visually using fairly common equipment, given that GCaMP3 signals can be observed easily on any fluorescence microscope with an appropriately narrow emission filter for eGFP. Thus dynamic signals can be observed *in situ* and in real time, including rapid signals such as those induced by cold shock or wounding. Furthermore, we demonstrate that signals from our GCaMP3 plants can be easily semi-quantified to allow for the characterization of signaling dynamics such as intensity and duration. Finally, we combine well-established *N. benthamiana* techniques such as virus-induced gene silencing (VIGS) and transient expression to demonstrate how these plants can be used to study both loss- and gain-of-function components in $Ca^{2+}$ signaling.

## Results

### Visualization and measurement of $Ca^{2+}$ signals in *Nicotiana* species

Using a conventional tissue culture method (Horsch et al. 1985, Clemente 2006), we transformed *N. benthamiana* and *N. tabacum* (nn and NN) with our GECI construct (*CaMV35S:GCaMP3*) using *Agrobacterium tumefaciens*. We identified multiple $T_2$ lines with clear expression of the *CaMV35S:GCaMP3* construct in each of our three genetic backgrounds by screening with fluorescence microscopy. While the GCaMP3 expression level (and thus basal fluorescence signals) varied between lines, we identified at least two lines in each background with relatively high signal and subsequently isolated homozygous individuals of each line for use in experiments. These transgenic lines show no detectable morphological changes relative to wild-type plants and develop and set seed normally. Confocal microscopy of transgenic lines showed clear expression of GCaMP3 in the cytosol and nucleus in both shoots and root tissue of *N. benthamiana* and *N. tabacum* (Supplementary Fig. S1).

While fluorescence microscopy images can be used for visualizing $Ca^{2+}$ signals, we also established a semi-quantitative method, that can be easily adapted to various applications, which relies on plate reader-based measurements of fluorescence from leaf discs. For all experiments, we treated leaf discs from a single leaf with both stimuli and water (or solvent-adjusted water, as appropriate) and normalized the fluorescence values as $F/F_{eq}$, where $F_{eq}$ was the average fluorescence of the final time point of water (control) samples (see the Materials and Methods for details on assay preparation), since the pre-treatment signals cannot be analyzed due to the lack of an injector system of our plate reader. $F_{eq}$ thus corresponded to the resting basal fluorescence signal. Using this assay, we were able to observe clear $Ca^{2+}$ elevation after treatment with ionomycin, a $Ca^{2+}$ ionophore (Supplementary Fig. S2). We then set out to assay $Ca^{2+}$ signals qualitatively and/or quantitatively in response to a variety of abiotic or biotic stimuli.

### Rapid wounding-induced $Ca^{2+}$ signals in *N. benthamiana*

We observed $Ca^{2+}$ signals in response to mechanical wounding in leaf tissue using fluorescence microscopy, and captured propagating signals in a 60 s time course (**Fig. 1A**). A spike in $Ca^{2+}$ was observed immediately in the cells local to the wounding site, followed by further $Ca^{2+}$ signaling that propagated through the adjacent vasculature to distal tissue, matching previous results with Arabidopsis (Beneloujaephajri et al. 2013, Kiep et al. 2015). One advantage of using *Nicotiana* species for experiments is their relatively large leaf area. We took advantage of this to test the effect of the established $Ca^{2+}$ channel blocker $GdCl_3$ to inhibit wound-related $Ca^{2+}$ signals by infiltrating leaves with either

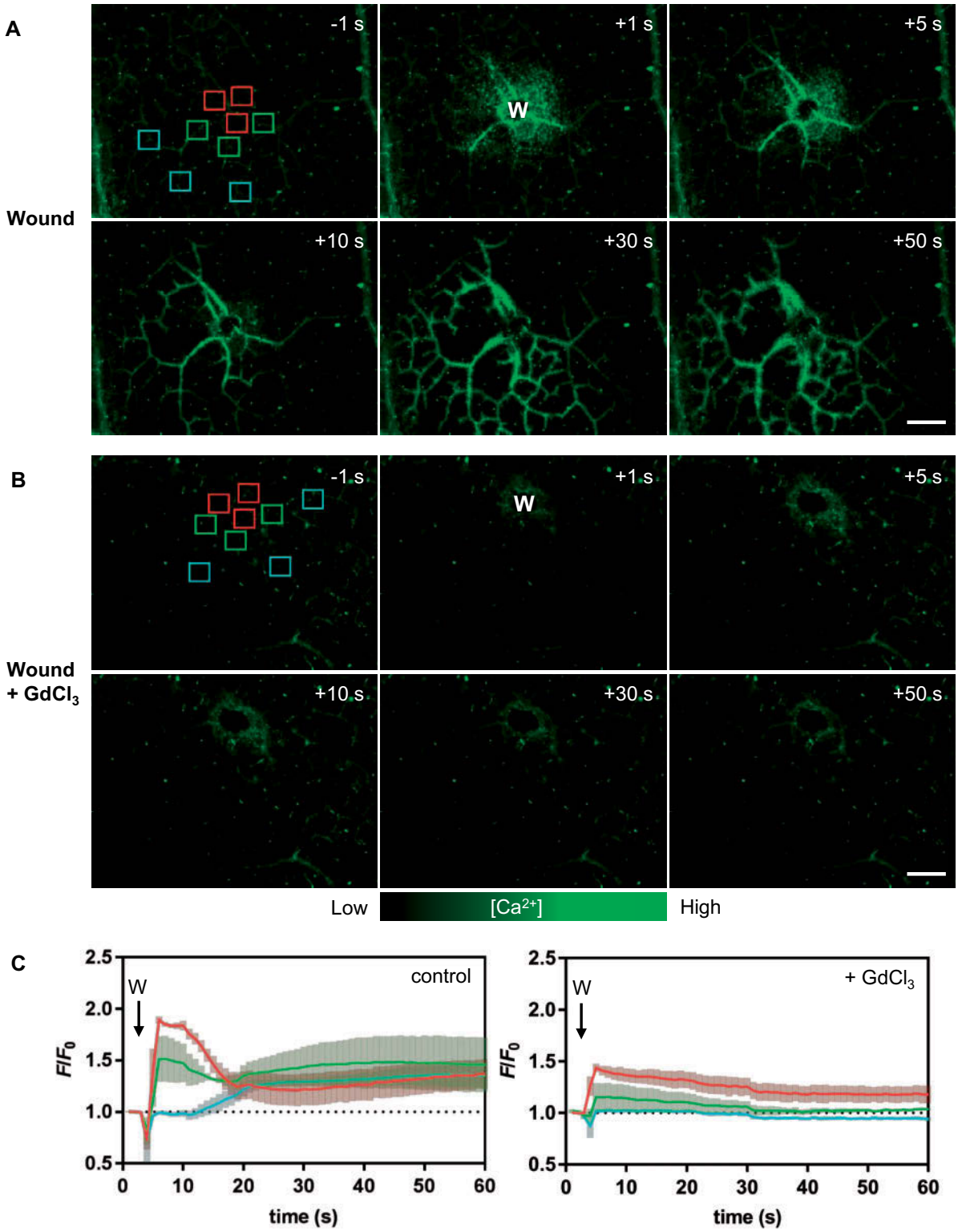


**Fig. 1** Wounding-induced local and vasculature $Ca^{2+}$ signals in *N. benthamiana*. Fluorescence microscopy showing GCaMP3 signal in response to wounding at the times indicated in the images (top right). Wounding was performed with forceps at the site marked (W) at 0 s. Scale bar = 1 mm. Leaves were pre-treated with (A) water or (B) 100 μM GdCl3. (C) Quantification of normalized ($F/F_0$) GCaMP3 signals in areas shown in −1 s panels of (A) and (B). Plotted values are the average of the three color-coded areas at the site of wounding (red), adjacent to the site of wounding (green) or distal to the site of wounding (blue). Arrows indicate the time of wounding, and the dashed line indicates the baseline signal ($F/F_0 = 1$). Error bars show ± SD.

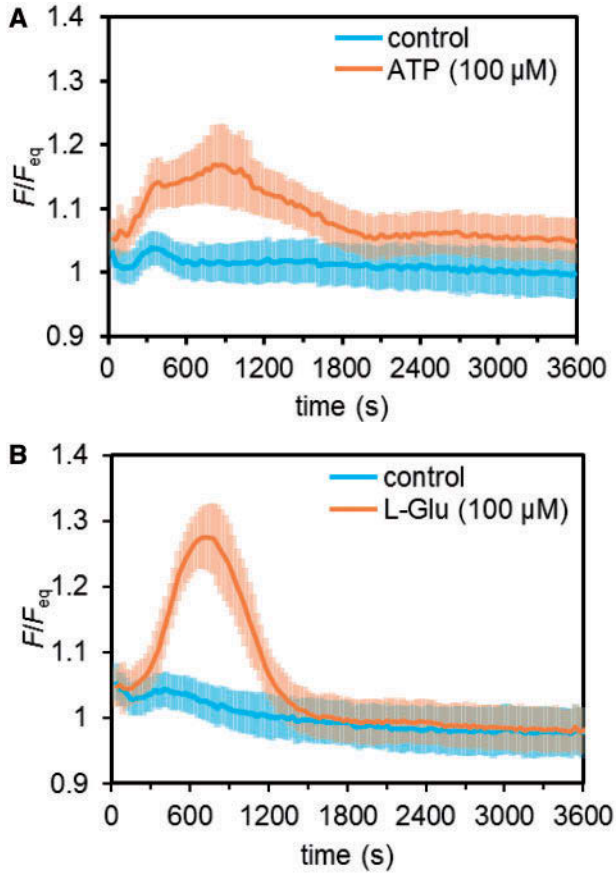


**Fig. 2** DAMP-triggered $Ca^{2+}$ signals in *N. benthamiana* leaf discs. GCaMP3 signal in response to exogenous application of (A) 100 µM ATP or (B) 100 µM L-glutamine in *N. benthamiana* leaf discs. In both (A) and (B), $ddH_2O$ was added as a negative control (blue). GCaMP3 signal was measured in leaf discs using a plate reader assay. Absolute fluorescence values for each experiment were normalized to the untreated control value as $F/F_{eq}$ (where $F$ was the measured fluorescence at a given time point and $F_{eq}$ was the averaged measurement for water-equilibrated control samples at the final resting time point measured). Averages of six replicate leaf discs ± SE are shown. The experiment has been conducted at least three times with similar results.

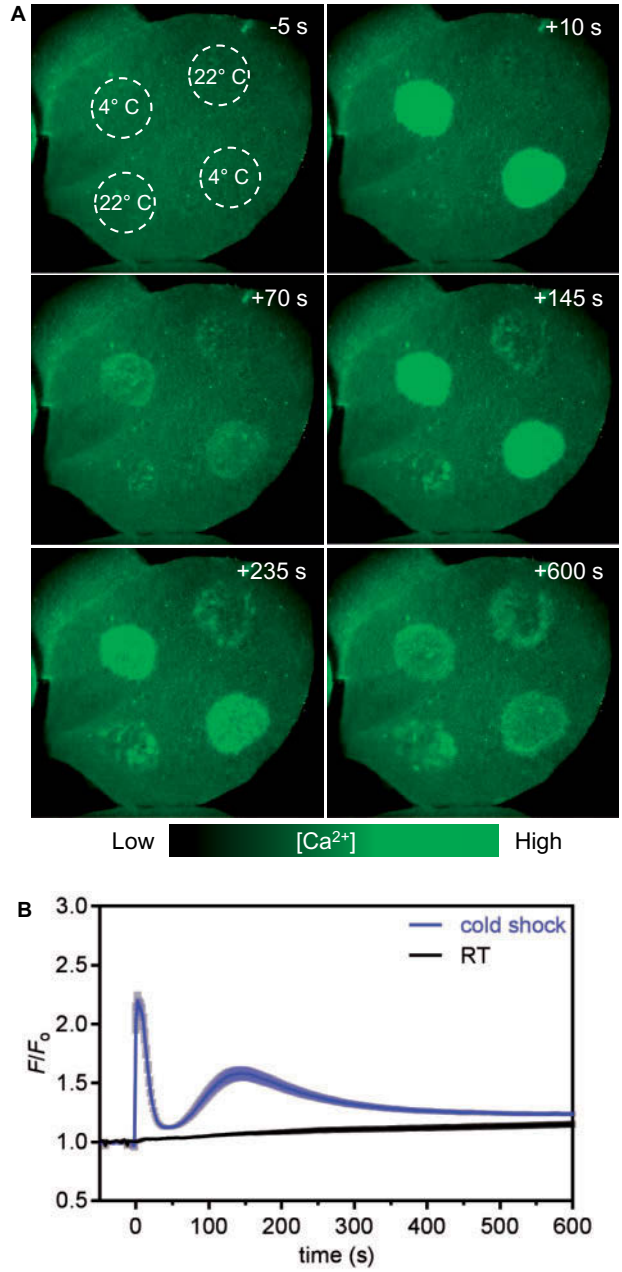


**Fig. 3** Cold shock induces a rapid, bi-phasic $Ca^{2+}$ burst in *N. benthamiana*. (A) Fluorescence microscopy showing GCaMP3 signal in response to cold (4°C) or room temperature (22°C) water droplets. Droplets were pipetted between −2 and +2 s onto the leaf surface at the positions indicated in the top left panel. Images show signal at the times indicated. (B) Quantification of signals shown in (A). Plotted values are averages of 12 regions of interest (ROIs) corresponding to areas treated with water at room temperature or 4°C, normalized to $F_0$. Errors bars show ± SE.

water of $GdCl_3$ prior to wounding. As shown in **Fig. 1B**, treatment with $GdCl_3$ inhibited wound-related $Ca^{2+}$ signals. Quantification of these signals confirmed the inhibition of wound-induced $Ca^{2+}$ signals at the site of wounding as well as signals within the vasculature by $Gd^{3+}$ (**Fig. 1C**).

Long-distance signaling in response to wounding is known to depend on members of the ionotropic glutamate receptor-like (GLR) channel family (Mousavi et al. 2013, Salvador-Recatalà et al. 2014, Salvador-Recatalà 2016). Additionally, various cellular compounds, including endogenous plant-derived peptides and ATP, have been studied as damage-associated molecular patterns (DAMPs) that can induce $Ca^{2+}$ signaling downstream of wounding or pathogen infection (Ranf et al. 2011, Tanaka et al. 2014;). As such we tested the effect of exogenous glutamate or ATP application on GCaMP3 signals in leaf discs, and were able to observe $Ca^{2+}$ signals induced by each (**Fig. 2**).

## Cold shock stress induces bi-phasic $Ca^{2+}$ signaling

$Ca^{2+}$ is known to mediate plant responses to abiotic stress such as chilling or cold shock (Knight et al. 1993, Chandra and Low 1997, Ma et al. 2015). As such we tested these treatments with our GCaMP3 transgenic plants using both fluorescence microscopy and our semi-quantification assays. In both assays we

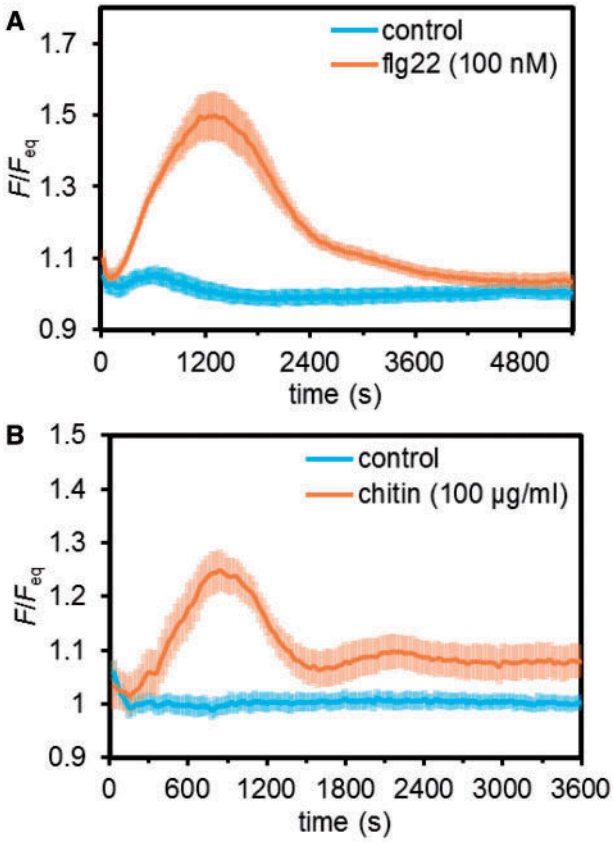


**Fig. 4** PAMP/MAMP-triggered $Ca^{2+}$ signals in *N. benthamiana*. Leaf discs were treated with (A) 100 nM flg22 or (B) 100 µg $ml^{-1}$ chitin. In both cases, $ddH_2O$ was used as a negative control (blue). GCaMP3 signal was measured in leaf discs using a plate reader assay. Plotted values show averages of six replicate leaf discs ± SE. The experiment has been conducted at least three times with similar results.

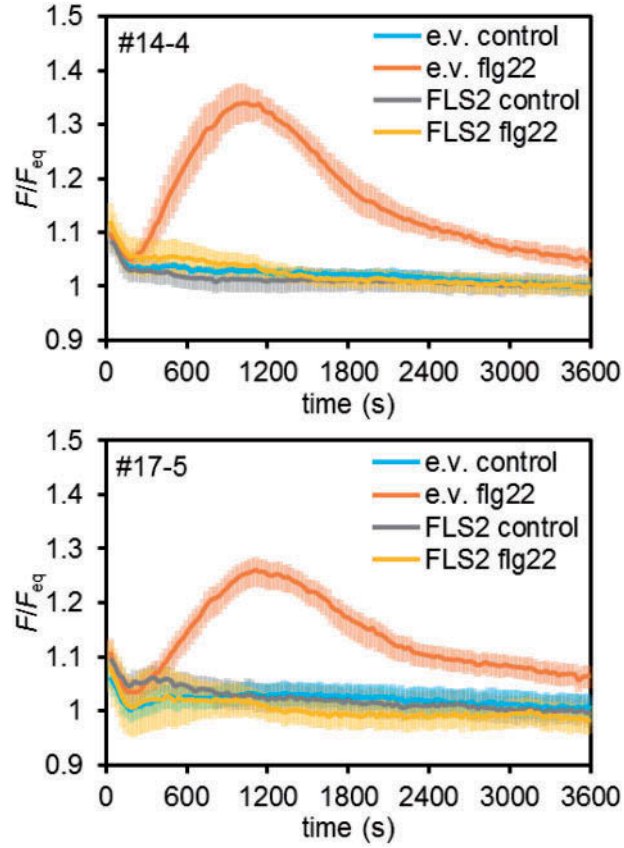


**Fig. 5** $Ca^{2+}$ signals in response to flg22 require the *Nb-FLS2* receptor. GCaMP3 signal in response to flg22 in *N. benthamiana* leaf discs from two GCaMP3-expressing lines (#14-4 or #17-5). Discs from 6-week-old plant leaves were taken 2 weeks after inoculation with *Agrobacterium* carrying TRV1 and either TRV2 empty vector (e.v.) or TRV2::*Nb-FLS2* (FLS2). Signals were measured for each after addition of $ddH_2O$ (control) or 100 nM flg22. GCaMP3 signal was measured in leaf discs using a plate reader assay. Averages of six replicate leaf discs ± SE are shown. Results are representative of multiple experiments.

observed rapid, bi-phasic $Ca^{2+}$ elevation in response to cold stress (Fig. 3; Supplementary Video S1), with an initial spike lasting 15–30 s, followed by a second signal peaking within 150 s of cold shock. Both peaks were measurable in both our microscopic analyses (Fig. 3A, B) and plate reader assays (Supplementary Fig. S3); however, our plate reader assays were only able to measure a single time point in the first peak, owing to a 15 s lag between treatment and initial measurement.

## PAMP-triggered $Ca^{2+}$ flux

In addition to wounding and abiotic stress, we also tested the effect of biotic stress-related stimuli on $Ca^{2+}$ via treatment with elicitors that are pathogen-/microbe-associated molecular patterns (PAMPs/MAMPs). Bacterial flagellin contains a well-studied 22 amino acid sequence (flg22) that activates PAMP-induced resistance in various plants (Zipfel 2008). Chitin, a polymer of *N*-acetyl D-glucosamine, is a major component of the fungal cell wall and is also a well-characterized PAMP (Liang et al. 2014). As shown in Fig. 4, flg22 and chitin were both able to induce robust $Ca^{2+}$ signals in our assay, in agreement with previous studies demonstrating that *N. benthamiana* possesses functional receptors for these PAMPs (Hann and Rathjen 2007, Gimenez-Ibanez et al. 2009).

## Silencing of endogenous *Nb-FLS2* suppresses flg22-induced $Ca^{2+}$ flux

To test the specificity of the flg22-induced signal in our GCaMP3 transgenic plants, we silenced the endogenous receptor for flg22 in *N. benthamiana*, *Nb-FLS2* (*Flagellin Sensing 2*) using VIGS (see Supplementary Fig. S4 for images of VIGS-silenced plants). While leaves from plants infected with *Tobacco rattle virus* 2 (TRV2) empty vector showed a normal $Ca^{2+}$ burst following application of flg22, leaves from plants *Nb-FLS2* silenced plants showed no response (Fig. 5), indicating the specificity of the $Ca^{2+}$ signal detected upon flg22 treatment.

## Pharmacological assays of flg22-induced $Ca^{2+}$ signals

We performed chemical inhibitor assays to evaluate further the flg22-induced $Ca^{2+}$ signals. Pre-treatment with the $Ca^{2+}$

channel blocker $GdCl_3$ significantly suppressed $Ca^{2+}$ signals in response to flg22 (Fig. 6A, B). Previous work has demonstrated important roles for both reactive oxygen species (ROS) and $Ca^{2+}$ release from internal stores during flg22-induced $Ca^{2+}$ signaling (Segonzac et al. 2011, Thor and Peiter 2014). In agreement with such previous work, we observed a significantly reduced flg22-induced peak signal in leaf discs pre-treated with either the NADPH oxidase inhibitor diphenyleneiodonium (DPI) (Fig. 6A, E) or neomycin, a phospholipase C (PLC) inhibitor that is generally used to inhibit $Ca^{2+}$ release from internal stores (Fig. 6A, C) (Peiter 2011). While DPI and neomycin treatment inhibited the flg22-induced peak signal (Fig. 6F), the timing of responses was unaffected (Fig. 6G). In contrast, pre-treatment with nifedipine had no clear effect on the flg22-induced signal magnitude, but did significantly alter the timing of the response (Fig. 6D, G), in agreement with previous work that demonstrated a delayed recovery in Arabidopsis PAMP-induced $Ca^{2+}$ signals following nifedipine treatment (Kwaaitaal et al. 2011). Thus our GCaMP3 plants represent an excellent tool to study the pharmacology of the amplitude and timing of PTI responses.

## Heterologous expression of Arabidopsis EFR can reconstitute perception of elf18 by *N. benthamiana*

Transient expression of a gene of interest by *Agrobacterium* infiltration is a particularly useful trait of *N. benthamiana* as a model system, and thus utilizing GCaMP3 transgenic plants to monitor $Ca^{2+}$ signals alongside transient expression is a promising tool for future research. To test this aspect, we performed transient expression of the Arabidopsis elongation factor-Tu (EF-Tu) receptor (*At-EFR*) in our GCaMP3 *N. benthamiana*. While the elf18 peptide from the conserved bacterial EF-Tu protein is a well-characterized PAMP in Arabidopsis, solanaceous plants such as *N. benthamiana* species lack its cognate receptor, EFR (Zipfel et al. 2006). As such, elf18 elicits no $Ca^{2+}$ signals in *N. benthamiana*, indicative of a lack of PTI induction by this PAMP. Leaves infiltrated with *Agrobacterium* carrying the HC-Pro silencing suppressor from *Tobacco etch virus* (TEV) alone thus showed no response to elf18 application (Fig. 7). Heterologous transient overexpression of the Arabidopsis elf18 receptor gene, *At-EFR*, however, was sufficient to reconstitute a modest but clear elf18-induced $Ca^{2+}$ burst (Fig. 7), matching previous findings that all components necessary for elf18 perception downstream of the receptor are present in solanaceae species (Zipfel et al. 2006, Lacombe et al. 2010).

## Functional analysis of transiently expressed ion channels via agroinfiltration

Cyclic nucleotide-gated channels (CNGCs) are non-selective cation channels represented by large families of isoforms in all plants examined to date (Mäser et al. 2001). Generally, CNGCs have been hypothesized to function as $Ca^{2+}$ channels in plants, and several isoforms have been empirically determined to be permeable to $Ca^{2+}$ or have $Ca^{2+}$-dependent phenotypes (Leng et al. 2002, Urquhart et al. 2007, Zhou et al. 2014, Charpentier et al. 2016, Gao et al. 2016). Recently, we examined the regulation of Arabidopsis CNGC12 and the related chimeric channel CNGC11/12 (Yoshioka et al. 2006) by CaM, and found that loss of an IQ-motif CaM-binding site could disrupt CNGC11/12-induced programmed cell death (PCD) (DeFalco et al. 2016). PCD induction by CNGC11/12 was previously shown to be $Ca^{2+}$ dependent (Urquhart et al. 2007) and so we tested whether our GCaMP3 system can measure elevated $Ca^{2+}$ levels induced by transient expression of CNGC11/12 using the *Agrobacterium* infiltration method.

While *Agrobacterium* itself caused an increase in autofluorescence (in non-transgenic *N. benthamiana*), expression of CNGC11/12 was able to induce a significant increase in the signal from our GCaMP3 plants above background levels, indicative of elevated $Ca^{2+}$ levels (Supplementary Fig. S5). $CNGC11/12^{DA}$ ($11/12^{I564D/Q565A}$, an IQ-motif mutant version) leads to a loss of channel function and PCD induction (DeFalco et al. 2016), and in keeping with this we observed no increase in GCaMP3 signal with expression of our $CNGC11/12^{DA}$ construct. While these measurements were performed prior to the onset of PCD [28 hours post-infiltration (h.p.i.)], PCD observations at later time points matched previous findings (Supplementary Fig. S5, right panel). These data indicated that our GCaMP3 *N. benthamiana* can also be utilized for the functional analysis of transiently expressed ion channels.

## *N. tabacum* GCaMP3 lines also respond to abiotic or biotic stimuli

While most experiments focused on our *N. benthamiana* GCaMP3 plants, we also tested responses to biotic or abiotic stimuli in our *N. tabacum* GCaMP3 lines. As was the case with *N. benthamiana*, *N. tabacum* leaves displayed biphasic $Ca^{2+}$ signals in response to cold shock, which were measurable by both microscopy and plate reader assays (Supplementary Fig. S6A and B, respectively). The DAMP signal, glutamate, also triggered a $Ca^{2+}$ signal in *N. tabacum* (Supplementary Fig. S6D). Both *N. tabacum* nn and NN also displayed similar $Ca^{2+}$ elevation following flg22 treatment compared with *N. benthamiana* (Supplementary Figs. 6C and 7, respectively).

# Discussion

The ability to monitor and measure $Ca^{2+}$ signals in real time is critical to understand complex responses to various stimuli. While no single method has yet proven ideal in every aspect, here we describe the development of a system that can be used with relative simplicity to observe a wide variety of $Ca^{2+}$ signals in *Nicotiana* species. The progenitor GCaMP sensor (Nakai et al. 2001) has subsequently been improved in terms of both basal and $Ca^{2+}$-responsive fluorescence (Tian et al. 2009), including the recently published derivative GCaMP6 (Chen et al. 2013); however, these sensors have not yet been utilized in plants. Here, we have used the third-generation GCaMP sensor to develop our *Nicotiana* sp. $Ca^{2+}$ analysis methods, with a focus on ease of use and adaptability to various assays. Other single-

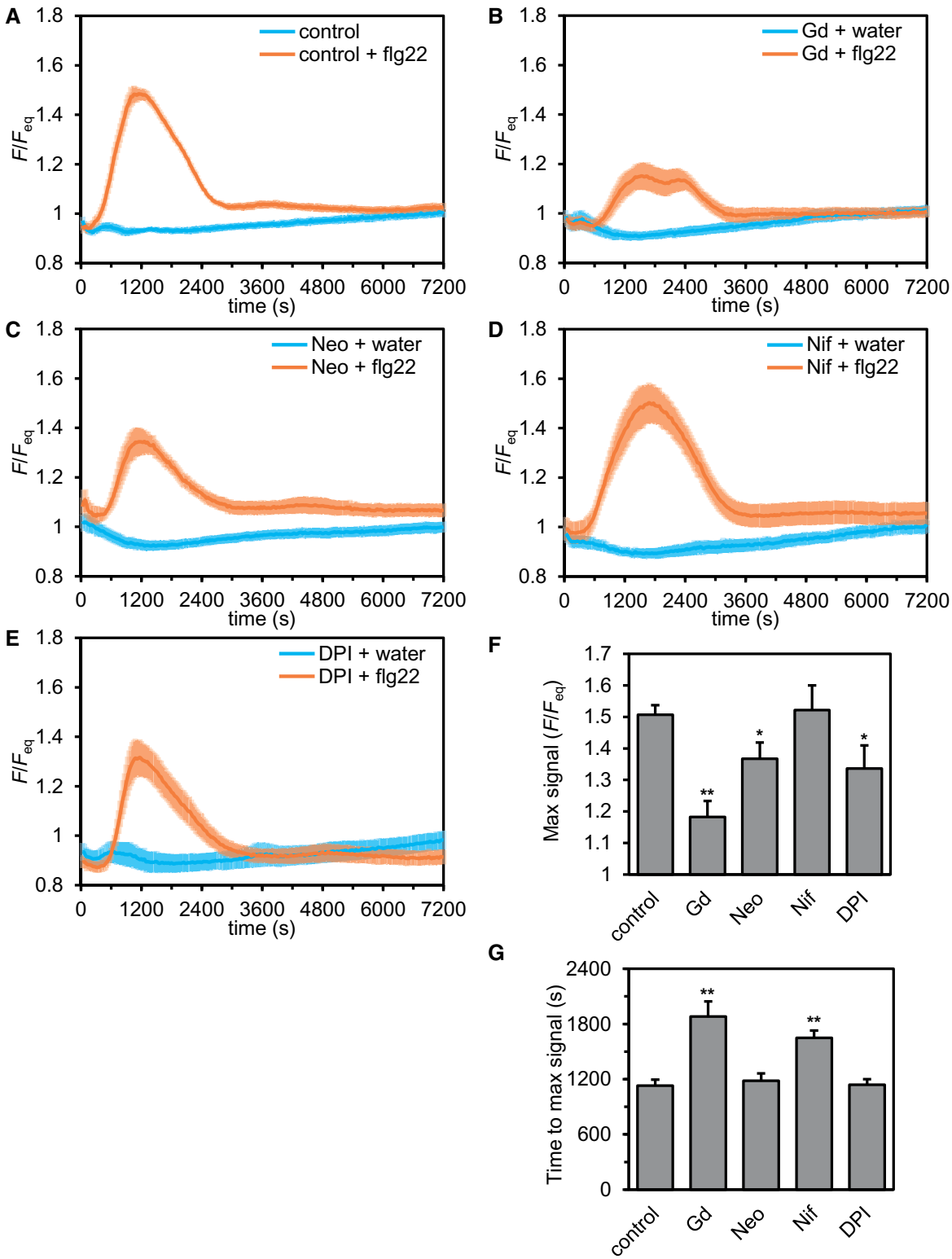


**Fig. 6** Internal $Ca^{2+}$ release and ROS are involved in flg22-induced $Ca^{2+}$ signals in *N. benthamiana*. Leaf discs from areas were equilibrated on $ddH_2O$ (A), 100 μM $GdCl_3$ (B), 100 μM neomycin (C), 100 μM nifedipine (D) or 100 μM DPI (E) prior to treatment with 100 nM flg22 (orange) or $ddH_2O$ as a negative control (blue). Plotted values were obtained by a plate reader with averages of six replicate leaf discs. Error bars show ± SE. (F and G) Maximum normalized signal (F) or time to maximum normalized signal (G) of each flg22-treated leaf disc from (A–E). GCaMP3 signal was measured in leaf discs using a plate reader. Error bars show ± SE. Values that were significantly different from control are indicated (*$P < 0.05$ or **$P < 0.005$, two-tailed *t*-test). The experiment has been conducted at least three times with similar results.

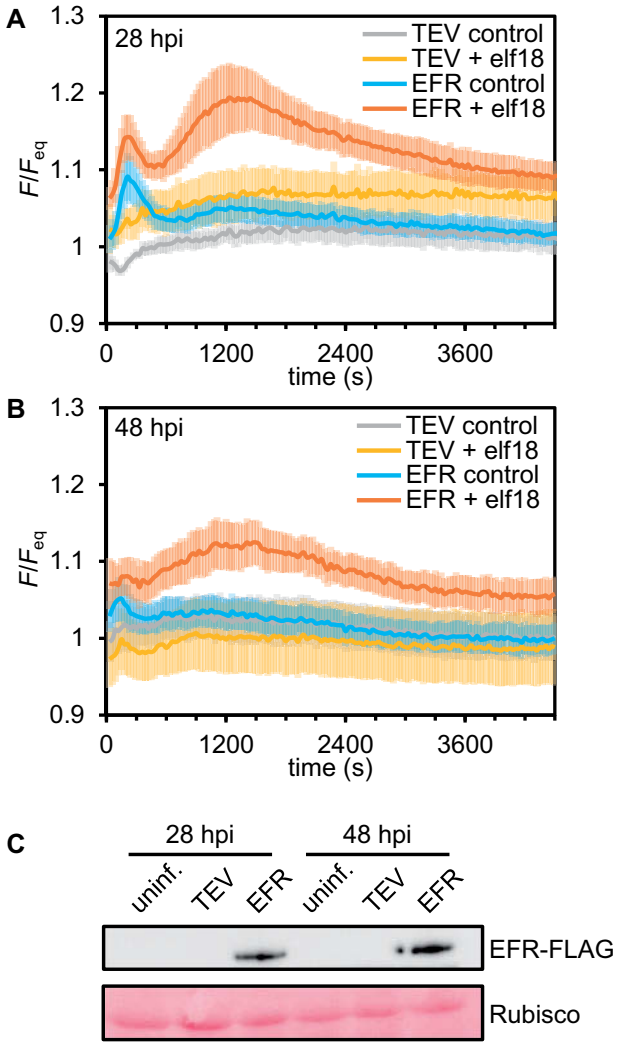


**Fig. 7** Transient expression of Arabidopsis *EFR* allows the induction of $Ca^{2+}$ signals in response to elf18 in *N. benthamiana*. GCaMP3 signal in response to elf18 in *N. benthamiana* leaf discs. Discs from 6-week-old plant leaves were treated with $ddH_2O$ (negative control) or 1 μM elf18 peptide (A) 28 or (B) 48 h after infiltration with *Agrobacterium*-carrying constructs as indicated. GCaMP3 signal was measured in leaf discs using a plate reader assay. Plotted values are averages of four leaf discs ± SE. (C) Western blot showing expression of EFR-FLAG at 28 or 48 h.p.i. Uninfiltrated leaf tissue (uninf.) and TEV are negative controls. Ponceau-S-stained Rubisco small subunit is shown as a loading control. Results are representative of multiple experiments.

wavelength sensors, including Cases and R-GECOs, have recently been adapted to plant studies, though primarily in the model plant Arabidopsis (Zhu et al. 2014, Keinath et al. 2015).

$Ca^{2+}$ has often been described as a central, ubiquitous or even universal second messenger in plants (Sanders et al. 2002, DeFalco et al. 2010, Kudla et al. 2010). Consistent with this view, and many previous studies, we observed and/or measured $Ca^{2+}$ spikes in response to abiotic or biotic stimuli. An advantage of using GCaMP3 as our indicator is the ease of use with microscopy, as exemplified by the ability to image the rapid (1 s) local $Ca^{2+}$ spike in the cells adjacent to the site of mechanical wounding, followed by signals in adjacent and subsequently distal vasculature (**Fig. 1**). Our wound-induced signals depended on the specific activity of $Ca^{2+}$-permeable channels, as these signals were blocked by $GdCl_3$ at the site of treatment (*i.e.* wounding) as well as at the vasculature system. It is of interest whether different types of channels are involved for primary and vasculature $Ca^{2+}$ signals, however (**Fig. 1B**). Ultimately, dissection of the components governing vasculature $Ca^{2+}$ signals requires additional high-resolution microscopy. We observed an elevation in GCaMP3 fluorescence in response to exogenous glutamate application (**Fig. 2**) as has been previously demonstrated in Arabidopsis (Dennison and Spalding 2000). ATP has also been identified as a DAMP in plants (Tanaka et al. 2014) and, consistent with previous findings, we also observed $Ca^{2+}$ signals upon treatment with exogenous ATP in our plate reader assay (**Fig. 2**).

Our *Nicotiana* GCaMP3 plants provide an excellent tool for the molecular analysis of $Ca^{2+}$ signaling dynamics in response to diverse stimuli. In particular, we validated the utility of both gene silencing by VIGS (**Fig. 5**) and heterologous transient expression (**Fig. 7**) in combination with our $Ca^{2+}$ indicator, and we believe such techniques will allow researchers to probe the roles of various molecular components in specific $Ca^{2+}$ signaling pathways with relative ease, without the production of numerous stable transgenic lines. This will be greatly aided by the recently completed draft sequence of the *N. benthamiana* genome (Bombarely et al. 2012) and ever-improving tools for the design of VIGS constructs (Fernandez-Pozo et al. 2015). While we validated our methods using well-characterized, differentially conserved receptors (*FLS2* and *EFR*), as more MAMP/PAMPs and their cognate receptors continue to be identified across diverse species (Mott et al. 2016, Wang et al. 2016), our GCaMP3 *N. benthamiana* and *N. tabacum* lines represent excellent tools to study the conservation of PTI signaling components. In addition, we have tested 10-day-old *N. benthamia* seedlings and succeeded in capturing flg22-induced signals, indicating the versatility of the system (Supplementary Fig. S8).

Chemical inhibitors can also provide important insights into the molecular components governing signaling responses. Our data (**Fig. 6**) corroborate a large body of previous work that has demonstrated the importance of mobilization of $Ca^{2+}$ from internal stores and ROS production in PAMP-induced $Ca^{2+}$ signaling (Lecourieux et al. 2005, Segonzac et al. 2011, Ranf et al. 2011, Thor and Peiter 2014).

The tobacco *N* gene encodes a nucleotide-binding leucine-rich repeat (NB-LRR)-type R protein, which confers resistance to TMV (Holmes 1954, Whitham et al. 1994, Erickson et al. 1999). While $Ca^{2+}$ transporter or $Ca^{2+}$-binding sensor proteins have been previously implicated in virus resistance (Anandalakshmi et al. 2000, Zhu et al. 2010, Nakahara et al. 2012), comparably little is currently known regarding the specifics of $Ca^{2+}$ signaling in responses to viral infection. Given that we have generated both cultivated tobacco (cv. Xanthi nn) and TMV-resistant (cv. Xanthi-nc NN) *N. tabacum* GCaMP3 lines (Supplementary Figs. S6, S7), these plants will be an excellent tool to study the roles of $Ca^{2+}$ signaling in mediating plant resistance to viruses. The hypersensitive response (HR) develops rapidly (approximately 48 h after inoculation with

TMV) in *N*-carrying tobacco (Erickson et al. 1999), and as such it will be illuminating to visualize $Ca^{2+}$ flux following viral infection in susceptible and resistant cultivars.

The iterative process of GECI improvement means that single-wavelength sensors are continually refined in terms of their signal and responsiveness (Helassa et al. 2015, Cho et al. 2017). We believe that generation of transgenic *Nicotiana* species with later generation GECI(s) will allow for the dissection of ever subtler aspects of $Ca^{2+}$ signaling, at ever greater spatio-temporal resolution.

## Materials and Methods

### Plant growth conditions

*Nicotiana benthamiana* and *N. tabacum* used for experiments were grown for approximately 6 weeks on Sunshine mix soil (Sun Gro Horticulture Canada) in a growth chamber under a 9/15 h light/dark regimen at 22°C (day) and 20°C (night) (60% relative humidity and 140 μE $m^{-2}$ $s^{-1}$). For seed production, 4-week-old plants were moved to a greenhouse room and grown under 16/8 h light/dark growth conditions at approximately 22°C (day) and 20°C (night).

### Generation of transgenic lines

*Nicotiana benthamiana* and *N. tabacum* were stably transformed via *Agrobacterium*-mediated transformation based on previously described methods (Horsch et al. 1985, Clemente 2006), with details as follows. *Agrobacterium tumefaciens* strain LBA4404 carrying the pBIN20::CaMV35S:GCaMP3 construct was cultured in 50 ml of YEP supplemented with antibiotics and 20 μM acetosyringone for 48–72 h at 28°C, 250 r.p.m. The culture was spun down and resuspended in 25 ml of co-cultivation medium (Clemente 2006) to a final $OD_{600}$ of approximately 0.5–1.0 and left at room temperature while preparing leaf tissue. Six- to eight-week-old leaves were cut into 4–8 $cm^2$ sections (avoiding the primary vein), and surface sterilized in 10% commercial bleach supplemented with one drop of Tween-20 per 50 ml for 10 min. Sterilized leaf sections were washed five times with sterile $ddH_2O$ and further cut into small (approximately 0.5 × 0.5 cm) explants. These explants were incubated with 25 ml of *Agrobacterium* suspension for 30 min with gentle agitation every 5–10 min. The leaf explants were blotted dry on sterile filter paper to remove excess *Agrobacterium*, then transferred (abaxial or adaxial side up) to solid co-cultivation medium (Clemente 2006). Following 2–3 d of co-cultivation, leaf explants were transferred to selection medium containing carbenicillin and cefotaxime (100 and 200 μg $ml^{-1}$, respectively) to eliminate bacteria and 50 μg $ml^{-1}$ kanamycin to select transformants (Clemente 2006). Regenerated transformants were then subcultured to 0.5 × MS agar (1% sucrose) medium to induce root formation. Following root formation, explants were potted in soil and grown to seed set. $T_2$ seed was collected and propagated to generate $T_3$ seed. Individuals from $T_3$ lines were screened based on fluorescence to identify homozygous $T_3$ lines. Introduced constructs were identified by PCR using the primers GCaMP3_F (5′-ATGGGTTCTCATCATCATCATC-3′) and GCaMP3_R (5′-TTACTTCGCTGTCATCATTTG-3′) for confirmation.

### Transient expression and virus-induced gene silencing (VIGS)

Transient expression was performed via infiltration with *A. tumefaciens* strain GV2260 as described previously (DeFalco et al. 2016). *Agrobacterium tumefaciens* carrying *CaMV35S:HC-Pro* from TEV was infiltrated alone or co-infiltrated with constructs as described in the figure legends. pB35GWF::*At-EFR*-FLAG was obtained from the Arabidopsis Biological Resource Center (ABRC clone # S5G20480BFF). VIGS experiments were performed as described previously (Liu et al. 2002, Segonzac et al. 2011). Two- to three-week old *N. benthamiana* plants were infected with *A. tumefaciens* carrying TRV1 and either TRV2 (empty vector), TRV2::Nb-*FLS2* or TRV2::*PDS*. Following infection, plants were monitored for approximately 3 weeks for signs of *phytoene desaturase* (*PDS*) silencing (bleaching of new leaves). Once silencing of *PDS* was consistent, corresponding leaves from TRV2 and TRV2::Nb-*FLS2* plants were used for experiments (see Supplementary Fig. S4).

### Protein extraction and Western blots

Protein samples were extracted from *N. benthamiana* leaf tissue by grinding in 20 mM Tris–HCl, 100 mM NaCl, 1 mM dithiothreitol (DTT), 1.25% Triton X-100, pH 8.0 and clarified via centrifugation at 6,000 × *g* at 4°C for 10 min. Clarified extracts were boiled in 1 × Laemmli loading buffer, separated by 12% SDS–PAGE and transferred to a polyvinylidene fluoride (PVDF) membrane. Blots were stained with Ponceau-S, blocked overnight at 4°C, and subsequently probed with αFLAG antisera (1 : 10,000 dilution). Immunoreactive bands were detected using Amersham ECL Prime Western Blotting Detection reagents (GE Healthcare) on a Chemidoc Touch Imaging System (Bio-Rad).

### Preparation of chemical stocks

ATP, $GdCl_3$ and neomycin were all dissolved in $ddH_2O$ as 1,000 × stocks. Ionomycin, DPI or nifedipine were each dissolved in dimethylsulfoxide (DMSO) to stock concentrations of 2, 10, or 20 mM, respectively. Chitin (Calbiochem) stocks were prepared fresh, by first grinding powder with a mortar and pestle for 5 min, after which a half-final volume of $ddH_2O$ was added and the mixture was ground for an additional 5 min. The resulting slurry was diluted to a final stock concentration of 10 mg $ml^{-1}$. L-Glutamate was prepared fresh for use in $ddH_2O$. flg22 and elf18 peptides were synthesized commercially and dissolved in $ddH_2O$, then diluted to 1,000 × stock.

### Semi-quantification of $Ca^{2+}$ signals and inhibitor assays

For each chemical treatment, 12 × 0.5 cm leaf discs from 6-week-old plants were equilibrated abaxial side up in 100 μl of $ddH_2O$ for 4–6 h in a Greiner 96-well flat black plate. Following equilibration, 100 μl of $ddH_2O$ (with or without addition of appropriate solvent) or chemical treatment was added to leaf discs, to final concentrations as indicated in the figure legends. GCaMP3 fluorescence was measured immediately following treatment employing a TECAN Infinite M1000 Pro plate-reader, using excitation at 470 nm (20 nm bandwidth) and emission detection at 525 nm (20 nm bandwidth). Measurements were recorded for each leaf disc at 30 s intervals, for total durations as indicated in the figures. Absolute fluorescence values for each experiment were normalized to the untreated control value as $F/F_{eq}$ (where $F$ was the measured fluorescence at a given time point and $F_{eq}$ was the averaged measurement for water-equilibrated control samples at the final resting time point measured). $F_{eq}$ was used due to a lack of injector system and, for this reason, all treatments and water controls were performed with leaf discs from the same leaf. Plotted values are averages of six replicate leaf discs, with the SE represented by error bars. For assays with chemical inhibitors, inhibitors were diluted in $ddH_2O$ to the concentrations described in the figures; leaf discs were equilibrated on the inhibitors (or $ddH_2O$ for control). Following equilibration, measurements were performed as described above.

### Real-time $Ca^{2+}$ imaging via fluorescence microscopy

Wounding measurements were recorded on a Leica M216F stereo fluorescence microscope using a Q Imaging Fast 1394 12-bit monochrome CCD camera controlled by OpenLab 5 software (Improvision Ltd.). GCaMP3 signal was visualized using the ET-GFP emission/excitation filter (Leica Microsystems). Images were captured every second during wounding experiments. Leaves were infiltrated with either water or 100 μM $GdCl_3$ 3–4 h prior to wounding experiments. Acquired images were semi-quantified using ImageJ.

Cold shock treatment leaves were imaged with a motorized fluorescence stereo microscope (SMZ-25, Nikon) equipped with a 1 × objective lens (P2-SHR Plan Apo, 0.156 NA, Nikon) and a highly sensitive sCMOS camera (ORCA-Flash0 V2, Hamamatsu Photonics). GCaMP3 was excited using a mercury lamp (motorized Intensilight Hg Illuminator, Nikon) and a GFP-B filter cube (Nikon) including a 460–500 nm excitation filter, a 505 nm dichroic mirror and a 510–560 nm fluorescent filter. GCaMP3 signal was acquired every 2 s and analyzed with microscope imaging software (NIS-Elements Advanced

Research, Nikon). A 5–10 µl aliquot of water (room temperature or 4°C) was applied onto the adaxial surface of a *Nicotiana* leaf.

## Accession numbers

Sequence data for genes referenced in this article can be found under the following accession numbers: *At-EFR* (At5g20480), *At-FLS2* (At5g46330), *Nb-FLS2* (Niben101Scf01785g10011) and *Nt-FLS2* (XM_016635313).

## Supplementary data

Supplementary data are available at PCP online.

## Funding

This study was supported by the Natural Sciences and Engineering Research Council (NSERC) [Discovery Grant to K.Y.]; the Japan Science and Technology Agency (JST) [PRESTO award to M.T.]; the National Science Foundation [MCB 1329723, IOS-1557899 to S.G.]; and the NSERC and the Ontario government [doctoral funding grants to T.A.D.].

## Acknowledgments

The authors thank Dr. Cyril Zipfel (The Sainsbury Laboratory, Norwich, UK) for kindly providing the *Nb-FLS2* silencing construct. The elf18 peptide was generously provided by Dr. G. Adam Mott and Dr. David S. Guttman (University of Toronto), while αFLAG antiserum was provided by Dr. Darrell Desveaux (University of Toronto). We also thank Ms. Zheng Song for technical assistance in generating transgenic plants. T.A.D., K.Y., M.T. and S.G. conceived the project. T.A.D. generated transgenic lines, and T.A.D., M.T., P.K. and V. P. performed experiments. T.A.D., W.M. and K.Y. wrote the article.

## Disclosures

The authors have no conflicts of interest to declare.

## References

Anandalakshmi, R., Marathe, R., Ge, X., Herr, J.M., Jr. Mau, C., Mallory, A., et al. (2000) A calmodulin-related protein that suppresses posttranscriptional gene silencing in plants. *Science* 290: 142–144.

Batistič, O. and Kudla, J. (2012) Analysis of calcium signaling pathways in plants. *Biochim. Biophys. Acta* 1820: 1283–1293.

Behera, S., Wang, N., Zhang, C., Schmitz-Thom, I., Strohkamp, S., Schültke, S., et al. (2015) Analyses of $Ca^{2+}$ dynamics using a ubiquitin-10 promoter-driven Yellow Cameleon 3.6 indicator reveal reliable transgene expression and differences in cytoplasmic $Ca^{2+}$ responses in Arabidopsis and rice (Oryza sativa) roots. *New Phytol.* 206: 751–760.

Beneloujaephajri, E., Costa, A., L'Haridon, F., Métraux, J.-P. and Binda, M. (2013) Production of reactive oxygen species and wound-induced resistance in Arabidopsis thaliana against Botrytis cinerea are preceded and depend on a burst of calcium. *BMC Plant Biol.* 13: 1–10.

Bombarely, A., Rosli, H.G., Vrebalov, J., Moffett, P., Mueller, L.A. and Martin, G.B. (2012) A draft genome sequence of Nicotiana benthamiana to enhance molecular plant–microbe biology research. *Mol. Plant Microbe Interact.* 25: 1523–1530.

Chandra, S. and Low, P.S. (1997) Measurement of $Ca^{2+}$ fluxes during elicitation of the oxidative burst in aequorin-transformed tobacco cells. *J. Biol. Chem.* 272: 28274–28280.

Charpentier, M., Sun, J., Martins, T.V., Radhakrishnan, G.V., Findlay, K., Soumpourou, E., et al. (2016) Nuclear-localized cyclic nucleotide–gated channels mediate symbiotic calcium oscillations. *Science* 352: 1102–1105.

Chen, T.-W., Wardill, T.J., Sun, Y., Pulver, S.R., Renninger, S.L., Baohan, A., et al. (2013) Ultrasensitive fluorescent proteins for imaging neuronal activity. *Nature* 499: 295–300.

Cho, J.-H., Swanson, C.J., Chen, J., Li, A., Lippert, L.G., Boye, S.E., et al. (2017) The GCaMP-R family of genetically encoded ratiometric calcium indicators. *ACS Chem. Biol.* (in press).

Choi, W.-G., Toyota, M., Kim, S.-H., Hilleary, R. and Gilroy, S. (2014) Salt stress-induced $Ca^{2+}$ waves are associated with rapid, long-distance root-to-shoot signaling in plants. *Proc. Natl. Acad. Sci. USA* 111: 6497–6502.

Clapham, D.E. (2007) Calcium signaling. *Cell* 131: 1047–1058.

Clemente, T. (2006) Nicotiana (Nicotiana tobaccum, Nicotiana benthamiana). *Methods Mol. Biol.* 343: 143–154.

DeFalco, T.A., Bender, K.W. and Snedden, W.A. (2010) Breaking the code: $Ca^{2+}$ sensors in plant signalling. *Biochem. J.* 425: 27–40.

DeFalco, T.A., Marshall, C.B., Munro, K., Kang, H.-G., Moeder, W., Ikura, M., et al. (2016) Multiple calmodulin-binding sites positively and negatively regulate Arabidopsis CYCLIC NUCLEOTIDE-GATED CHANNEL 12. *Plant Cell* 28: 1738–1751.

Dennison, K.L. and Spalding, E.P. (2000) Glutamate-gated calcium fluxes in Arabidopsis. *Plant Physiol.* 124: 1511–1514.

Erickson, F.L., Dinesh-Kumar, S.P., Holzberg, S., Ustach, C.V., Dutton, M., Handley, V., et al. (1999) Interactions between tobacco mosaic virus and the tobacco N gene. *Philos. Trans. R. Soc. B: Biol. Sci.* 354: 653–658.

Fernandez-Pozo, N., Rosli, H.G., Martin, G.B. and Mueller, L.A. (2015) The SGN VIGS tool: user-friendly software to design virus-induced gene silencing (VIGS) constructs for functional genomics. *Mol. Plant* 8: 486–488.

Gao, Q.-F., Gu, L.-L., Wang, H.-Q., Fei, C.-F., Fang, X., Hussain, J., et al. (2016) Cyclic nucleotide-gated channel 18 is an essential $Ca^{2+}$ channel in pollen tube tips for pollen tube guidance to ovules in Arabidopsis. *Proc. Natl. Acad. Sci. USA* 113: 3096–3101.

Gilroy, S., Hughes, W.A. and Trewavas, A.J. (1989) A comparison between Quin-2 and aequorin as indicators of cytoplasmic calcium levels in higher plant cell protoplasts. *Plant Physiol.* 90: 482–491.

Gimenez-Ibanez, S., Hann, D.R., Ntoukakis, V., Petutschnig, E., Lipka, V. and Rathjen, J.P. (2009) AvrPtoB targets the LysM receptor kinase CERK1 to promote bacterial virulence on plants. *Curr. Biol.* 19: 423–429.

Goodin, M.M., Zaitlin, D., Naidu, R.A. and Lommel, S.A. (2008) Nicotiana benthamiana: its history and future as a model for plant-pathogen interactions. *Mol. Plant Microbe Interact.* 21: 1015–1026.

Grynkiewicz, G., Poenie, M. and Tsien, R.Y. (1985) A new generation of $Ca^{2+}$ indicators with greatly improved fluorescence properties. *J. Biol. Chem.* 260: 3440–3450.

Hann, D.R. and Rathjen, J.P. (2007) Early events in the pathogenicity of Pseudomonas syringae on Nicotiana benthamiana. *Plant J.* 49: 607–618.

Helassa, N., Zhang, X.H., Conte, I., Scaringi, J., Esposito, E., Bradley, J., et al. (2015) Fast-response calmodulin-based fluorescent indicators reveal rapid intracellular calcium dynamics. *Sci. Rep.* 5: 15978.

Holmes, F.O. (1954) Inheritance of resistance to viral diseases in plants. *Adv. Virus Res.* 2: 1–31.

Horsch, R.B., Fry, J.E., Hoffman, N.L., Wallroth, M., Eichholtz, D.Z., Rogers, S.G., et al. (1985) A simple and general method for transferring genes into plants. *Science* 227: 1229—1231.

Keinath, N.F., Waadt, R., Brugman, R., Schroeder, J.I., Grossmann, G., Schumacher, K., et al. (2015) Live cell imaging with R-GECO1 sheds light on flg22- and chitin-induced transient [$Ca^{2+}$]cyt patterns in Arabidopsis. *Mol. Plant* 8: 1188–1200.

Kiep, V., Vadassery, J., Lattke, J., Maaß, J.P., Boland, W., Peiter, E., et al. (2015) Systemic cytosolic $Ca^{2+}$ elevation is activated upon wounding and herbivory in Arabidopsis. *New Phytol.* 207: 996–1004.

Knight, H. and Knight, M.R. (1995) Recombinant aequorin methods for intracellular calcium measurement in plants. *Methods Cell Biol.* 49: 201–216.

Knight, M.R., Read, N.D., Campbell, A.K. and Trewavas, A.J. (1993) Imaging calcium dynamics in living plants using semi-synthetic recombinant aequorins. *J. Cell Biol.* 121: 83–90.

Krebs, M., Held, K., Binder, A., Hashimoto, K., Den Herder, G., Parniske, M., et al. (2012) FRET-based genetically encoded sensors allow high-resolution live cell imaging of $Ca^{2+}$ dynamics. *Plant J.* 69: 181–192.

Kudla, J., Batistic, O. and Hashimoto, K. (2010) Calcium signals: the lead currency of plant information processing. *Plant Cell* 22: 541–563.

Kwaaitaal, M., Huisman, R., Maintz, J., Reinstadler, A., Panstruga, R., Reinstädler, A., et al. (2011) Ionotropic glutamate receptor (iGluR)-like channels mediate MAMP-induced calcium influx in Arabidopsis thaliana. *Biochem. J.* 440: 355–365.

Lacombe, S., Rougon-Cardoso, A., Sherwood, E., Peeters, N., Dahlbeck, D., van Esse, H.P., et al. (2010) Interfamily transfer of a plant pattern-recognition receptor confers broad-spectrum bacterial resistance. *Nat. Biotechnol.* 28: 365–369.

Lecourieux, D., Lamotte, O., Bourque, S., Wendehenne, D., Mazars, C., Ranjeva, R., et al. (2005) Proteinaceous and oligosaccharidic elicitors induce different calcium signatures in the nucleus of tobacco cells. *Cell Calcium* 38: 527–538.

Leng, Q., Mercier, R.W., Hua, B.-G., Fromm, H. and Berkowitz, G.A. (2002) Electrophysiological analysis of cloned cyclic nucleotide-gated ion channels. *Plant Physiol.* 128: 400–410.

Liang, Y., Tóth, K., Cao, Y., Tanaka, K., Espinoza, C. and Stacey, G. (2014) Lipochitooligosaccharide recognition: an ancient story. *New Phytol.* 204: 289–296.

Liu, Y.L., Schiff, M. and Dinesh-Kumar, S.P. (2002) Virus-induced gene silencing in tomato. *Plant J.* 31: 777–786.

Ma, Y., Dai, X., Xu, Y., Luo, W., Zheng, X., Zeng, D., et al. (2015) COLD1 confers chilling tolerance in rice. *Cell* 160: 1209–1221.

Mäser, P., Thomine, S., Schroeder, J.I., Ward, J.M., Hirschi, K., Sze, H., et al. (2001) Phylogenetic relationships within cation transporter families of Arabidopsis. *Plant Physiol.* 126: 1646–1667.

Miyawaki, A., Llopis, J., Heim, R., McCaffery, J.M., Adams, J.A., Ikura, M., et al. (1997) Fluorescent indicators for $Ca^{2+}$ based on green fluorescent proteins and calmodulin. *Nature* 388: 882–887.

Monshausen, G.B. (2012) Visualizing $Ca^{2+}$ signatures in plants. *Curr. Opin. Plant Biol.* 15: 677–682.

Mott, G.A., Thakur, S., Smakowska, E., Wang, P.W., Belkhadir, Y., Desveaux, D., et al. (2016) Genomic screens identify a new phytobacterial microbe-associated molecular pattern and the cognate Arabidopsis receptor-like kinase that mediates its immune elicitation. *Genome Biol.* 17: 98.

Mousavi, S.A.R., Chauvin, A., Pascaud, F., Kellenberger, S. and Farmer, E.E. (2013) GLUTAMATE RECEPTOR-LIKE genes mediate leaf-to-leaf wound signalling. *Nature* 500: 422–426.

Nagai, T., Yamada, S., Tominaga, T., Ichikawa, M. and Miyawaki, A. (2004) Expanded dynamic range of fluorescent indicators for $Ca^{2+}$ by circularly permuted yellow fluorescent proteins. *Proc. Natl. Acad. Sci. USA* 101: 10554–10559.

Nakahara, K.S., Masuta, C., Yamada, S., Shimura, H., Kashihara, Y., Wada, T.S., et al. (2012) Tobacco calmodulin-like protein provides secondary defense by binding to and directing degradation of virus RNA silencing suppressors. *Proc. Natl. Acad. Sci. USA* 109: 10113–10118.

Nakai, J., Ohkura, M. and Imoto, K. (2001) A high signal-to-noise $Ca^{2+}$ probe composed of a single green fluorescent protein. *Nat. Biotechnol.* 19: 137–41.

Peiter, E. (2011) The plant vacuole: emitter and receiver of calcium signals. *Cell Calcium* 50: 120–128.

Ranf, S., Eschen-Lippold, L., Pecher, P., Lee, J. and Scheel, D. (2011) Interplay between calcium signalling and early signalling elements during defence responses to microbe- or damage-associated molecular patterns. *Plant J.* 68: 100–113.

Rose, T., Goltstein, P.M., Portugues, R. and Griesbeck, O. (2014) Putting a finishing touch on GECIs. *Front. Mol. Neurosci.* 7: 88.

Salvador-Recatalà, V. (2016) New roles for the GLUTAMATE RECEPTOR-LIKE 3.3, 3.5, and 3.6 genes as on/off switches of wound-induced systemic electrical signals. *Plant Signal. Behav.* 11: e1161879.

Salvador-Recatalà, V., Tjallingii, W.F. and Farmer, E.E. (2014) Real-time, in vivo intracellular recordings of caterpillar-induced depolarization waves in sieve elements using aphid electrodes. *New Phytol.* 203: 674–684.

Sanders, D., Pelloux, J., Brownlee, C. and Harper, J.F. (2002) Calcium at the crossroads of signaling. *Plant Cell* 14: 401–418.

Segonzac, C., Feike, D., Gimenez-Ibanez, S., Hann, D.R., Zipfel, C. and Rathjen, J.P. (2011) Hierarchy and roles of pathogen-associated molecular pattern-induced responses in Nicotiana benthamiana. *Plant Physiol.* 156: 687–99.

Sieberer, B.J., Chabaud, M., Timmers, A.C.J., Monin, A.A.A., Fournier, J.J. and Barker, D.G. (2009) A nuclear-targeted cameleon demonstrates intranuclear $Ca^{2+}$ spiking in Medicago truncatula root hairs in response to rhizobial nodulation factors. *Plant Physiol* 151: 1197–1206.

Souslova, E.A., Belousov, V.V., Lock, J.G., Strömblad, S., Kasparov, S., Bolshakov, A.P., et al. (2007) Single fluorescent protein-based $Ca^{2+}$ sensors with increased dynamic range. *BMC Biotechnol.* 7: 37.

Steinhorst, L. and Kudla, J. (2013) Calcium—a central regulator of pollen germination and tube growth. *Biochim. Biophys. Acta* 1833: 1573–1581.

Tanaka, K., Choi, J., Cao, Y. and Stacey, G. (2014) Extracellular ATP acts as a damage-associated molecular pattern (DAMP) signal in plants. *Front. Plant Sci.* 5: 446.

Thor, K. and Peiter, E. (2014) Cytosolic calcium signals elicited by the pathogen-associated molecular pattern flg22 in stomatal guard cells are of an oscillatory nature. *New Phytol.* 204: 873–881.

Tian, L., Hires, S.A. and Looger, L.L. (2012) Imaging neuronal activity with genetically encoded calcium indicators. *Cold Spring Harb. Protoc.* 7: 647–656.

Tian, L., Hires, S.A., Mao, T., Huber, D., Chiappe, M.E., Chalasani, S.H., et al. (2009) Imaging neural activity in worms, flies and mice with improved GCaMP calcium indicators. *Nat. Methods* 6: 875–881.

Toyota, M., Furuichi, T., Sokabe, M. and Tatsumi, H. (2013) Analyses of a gravistimulation-specific $Ca^{2+}$ signature in Arabidopsis using parabolic flights. *Plant Physiol.* 163: 543–554.

Toyota, M., Furuichi, T., Tatsumi, H. and Sokabe, M. (2007) Cytoplasmic calcium increases in response to changes in the gravity vector in hypocotyls and petioles of Arabidopsis seedlings. *Plant Physiol.* 146: 505–514.

Urquhart, W., Gunawardena, A.H., Moeder, W., Ali, R., Berkowitz, G.A. and Yoshioka, K. (2007) The chimeric cyclic nucleotide-gated ion channel ATCNGC11/12 constitutively induces programmed cell death in a $Ca^{2+}$ dependent manner. *Plant Mol. Biol.* 65: 747–761.

Wang, L., Albert, M., Einig, E., Fürst, U., Krust, D. and Felix, G. (2016) The pattern recognition receptor CORE of Solanaceae detects bacterial cold shock protein. *Nat. Plants* 2: 1–9.

Whitaker, M. (2012) Genetically-encoded probes for measurement of intracellular calcium. *Methods Cell Biol.* 99: 153–182.

Whitham, S., Dinesh-Kumar, S.P., Choi, D., Hehl, R., Corr, C. and Baker, B. (1994) The product of the tobacco mosaic virus resistance gene N: similarity to Toll and the interleukin-1 receptor. *Cell* 78: 1101–1115.

Yoshioka, K., Moeder, W., Kang, H.-G., Kachroo, P., Masmoudi, K., Berkowitz, G., et al. (2006) The chimeric Arabidopsis CYCLIC NUCLEOTIDE-GATED ION CHANNEL11/12 activates multiple pathogen resistance responses. *Plant Cell* 18: 747–763.

Zhou, L., Lan, W., Jiang, Y., Fang, W. and Luan, S. (2014) A calcium-dependent protein kinase interacts with and activates a calcium channel to regulate pollen tube growth. *Mol. Plant* 7: 369–376.

Zhu, X., Caplan, J., Mamillapalli, P., Czymmek, K. and Dinesh-Kumar, S.P. (2010) Function of endoplasmic reticulum calcium ATPase in innate immunity-mediated programmed cell death. *EMBO J.* 29: 1007–1018.

Zhu, X., Taylor, A., Zhang, S., Zhang, D., Feng, Y., Liang, G., et al. (2014) Measuring spatial and temporal $Ca^{2+}$ signals in Arabidopsis plants. *J. Vis. Exp.* e51945.

Zipfel, C. (2008) Pattern-recognition receptors in plant innate immunity. *Curr. Opin. Immunol.* 20: 10–16.

Zipfel, C., Kunze, G., Chinchilla, D., Caniard, A., Jones, J.D.G., Boller, T., et al. (2006) Perception of the bacterial PAMP EF-Tu by the receptor EFR restricts Agrobacterium-mediated transformation. *Cell* 125: 749–760.